IOP Publishing Physica Scripta
Phys. Scr. 95 (2020) 045804 (10pp) https://doi.org/10.1088/1402-4896/ab5ca0

The gamma radiation effect on the surface morphology and optical properties of alpha-methyl curcumin: PMMA film

Jabbar H Jebur[1], Qusay M A Hassan[1], Mohammed F Al-Mudhaffer[1], Ahmed S Al-Asadi[1], Rita S Elias[2], Bahjat A Saeed[3] and C A Emshary[1]

[1] Department of Physics, College of Education for Pure Sciences, University of Basrah, Basrah, Iraq
[2] College of Pharmacy, University of Basrah, Basrah, Iraq
[3] Department of Chemistry, College of Education for Pure Sciences, University of Basrah, Basrah, Iraq

E-mail: qusayali64@yahoo.co.in

Received 28 August 2019, revised 14 November 2019
Accepted for publication 28 November 2019
Published 12 February 2020

Abstract

The effect of gamma, γ, radiation on the surface morphology and the optical properties of a prepared alpha-methyl curcumin: PMMA film were studied under different doses (7, 14, 21 and 28 Gy) of γ-rays emitted by ^{137}Cs source. To monitor the effect of γ radiation on the prepared sample, the UV–visible absorbance and transmittance measurements of the pristine and the irradiated sample were carried out in the spectral range 400–900 nm at room temperature. An optical microscope and image J software were utilized to examine any changes in the surface morphology for the pre and post irradiated samples. The obtained results indicated that the surface morphology, linear and nonlinear optical properties of the films have been affected by γ radiation.

Keywords: gamma-ray, surface morphology, optical constants, nonlinear optical properties, UV–visible spectra

(Some figures may appear in colour only in the online journal)

1. Introduction

During the past four decades, the search for materials possessing high nonlinear optical properties is a continuous issue due to their importance. Materials that have high nonlinear optical properties shows efficient performances in various photonic applications, viz., data storage [1, 2], optical bistability [3], optical switching [4], optical limiting [5–7], optical phase conjugation [8] etc. Most of these applications depends on the third-order nonlinear optical susceptibility, $\chi^{(3)}$, (the real and imaginary parts), the nonlinear refractive index, n_2, and the nonlinear absorption coefficient, β. The researchers in this field followed two paths to find materials having such properties, the first is the study of the nonlinear optical properties of the existing and known materials such as the dye solutions [9], the dye doped polymer films [10], the vegetable oils [11–14], the metal oils [15–18], the single crystals [19], the liquid crystals, [20] the nanoparticle composites [21] etc. Researchers have also been working on the manufacturing and synthesis of new materials for the same purposes, such as the phthalocyanine compounds [22, 23], the curcuminoids compounds [24–27], etc. The second path was to develop the nonlinear optical properties of the materials by studying the effect of many parameters on their properties such as the effect of the concentration [28], the wavelength [29], the incident intensity [30], the temperature [31], the salt concentration [32], the glucose concentration [33], the pH concentration [34] to name a few.

Owing to the development of radiation techniques during the last fifteen years such as the use of gamma, γ, radiation intensive researches have been directed towards the improvements of various properties of number of materials. Machnowski *et al* [35] have studied the effect of γ-ray on the mechanical properties and susceptibility to biodegradation of natural fibers. Rani *et al* [36] studied the effect of γ-ray on structural and thermal properties of hydroxyl propyl methyl

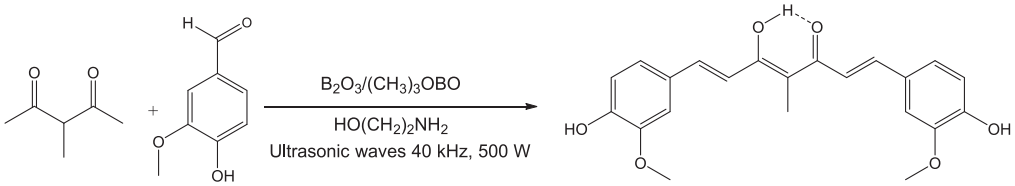

Figure 1. Synthesis of the alpha-methyl curcumin.

cellulose polymer. Eid *et al* [37] studied the effect of γ-ray on the optical energy gap of poly(Vinyl Alcohole). Brostow *et al* [38] studied the effect of γ-ray on polystyrene. Arshak and Korostynska [39] studied the effect of γ-ray on tellurium dioxide. Martel-Estrada *et al* [40] studied the effect of γ-ray on the thermal properties of chitosan. Darwish *et al* [41] have studied the effect of γ-ray on the structural, electrical and optical properties of nanostructure thin films of nickel phthalocyanine. Kilic *et al* [42] studied the effect of γ-ray on the mechanical and dielectric properties of volcanic basalt. Tahir [43] studied the effect of γ-ray on the optical properties of Cds thin films and Song *et al* [44] studied the effect of γ-ray on the properties of aluminum dihydrogen triphosphate. Ramya *et al* [45] studied the effect of γ-ray on enhancing magnetic behavior and cell proliferation dual metal ions. Al Harbi and Aly [46] studied the effect of γ-ray dose on the optical properties of $(AsTe)_x(GeSe_2)_{100-x}(x = 5)$ thin films. Mustapha *et al* [47] find out the influence of γ-ray onto transparent indium tin oxide thin films and Babu *et al* [48] studied the effect of γ-ray on the structural optical and electrical properties of nanostructured CdHgTe thin films and Salari *et al* [49] studied the effect of γ-ray on structural and surface properties of ZnO thin films. Ramya *et al* [50] studied the effect of γ-ray on (methyl methacrylate)-reduced graphene oxide composite thin films for multi-functional applications and Paula *et al* [51] studied the effect of γ-ray on polycaprolactone/zinc oxide nanocomposite films. Karmaker *et al* [52] studied the effect of γ-ray on the fabrication and characterization of PVA-gelatin-nano crystalline cellulose, Elamin *et al* [53] studied the effect of γ-ray on the optical properties of TiO_2 and ZnO thin films and Nabiyev *et al* [54] studied the effect of γ-ray on the morphological properties of HDPE+% ZrO_2 polymer nanocomposites.

The current work aims to synthesis of a new organic material with high nonlinear optical properties, as well as improves these properties by exposing it to gamma (γ) radiation. To achieve this goal, one of the curcumin compounds was prepared since curcumin has high nonlinear optical properties [24, 26, 27]. Curcumin is the yellow pigment that is responsible for the yellow color of the root of the plant curcuma longa *L* [55]. It has been shown to exhibit a wide range of biological activities the most prominent amongst are the anticancer, anti-inflammatory, antioxidant and the antibacterial [56–58]. Curcumin can exist as a tautomeric mixture of the enol and the diketo tautomers with the enol form as the major component in both the solid state and solution [59]. The enol form is the tautomer that is responsible for the long wavelength band appears near 430 nm in the electronic spectrum of the curcumin [60]. It has been shown that the addition of water to the ethanolic solution of curcumin shifts the tautomeric equilibrium towards the diketo form giving rise to a new band in its spectrum at 355 nm [61]. This may suggest that the major optical properties of curcumin are due to its enolic form.

In this work, the surface morphology, the linear and the nonlinear optical properties of the alpha-methyl curcumin: PMMA film are investigated using an optical microscope, image J software, and spectra measurements. The effect of the γ radiation on the surface morphology, the linear and the nonlinear optical properties of the alpha-methyl curcumin: PMMA film are reported. The extinction coefficient, k, the refractive index, n, the real, ε_1, and imaginary, ε_2, parts of the dielectric constant, the nonlinear refractive index, n_2, the linear optical susceptibility, $\chi^{(1)}$ and the third-order nonlinear optical susceptibility, $\chi^{(3)}$ for the pristine and the γ-irradiated sample are determined.

2. Experimental

2.1. Synthesis of alpha-methyl curcumin

The alpha-methyl curcumin compound was prepared according to Lei *et al* [62]. In a 100 ml round-bottomed flask a mixture of boron oxide (1.81 g, 0.026 mol), monoethanolamine (0.74 ml), trimethyl borate (4 ml) and DMF (12 ml) were placed. To this mixture a mixture of vaniline (7.60 g, 0.05 mol) and 3-methyl-2, 4-pentanedione (2.97 g, 0.026 mol) was added. The reaction flask was placed in an ultrasonic cleaner (40 kHz, 500 W) and the reaction mixture was irradiated at 80 °C for 30 min. At the end of the reaction, the mixture was poured onto a 200 ml of warmed acetic acid (5% V/V). Post filtration of the crude product it was chromatographically separated on a 200–300 mesh silica gel using petroleum ether/diethyl ether (2:1) as an eluent. Alpha -methyl curcumin was obtained as yellow powder mp. 186°C–187°C. IR (KBr disc) cm^{-1}: 2926, 1626,1598, 1458, 949,787; ^1H NMR ($CDCl_3$) (tautomeric mixture of enol and diketo forms) δ: 17.2 (s, 1H, chelated –OH), 7.96–6.69 (m, 10H, Ar-H + –CH=CH–), 5.90 and 5.84 (s, 2H, OH), 4.20 (s, 1H,=CH–), 3.95 and 3.93 (s, 1H, $-OCH_3$), 2.16 and 1.50 (s, 1H, $-CH_3$). The purity of the studied compound was checked by its elemental analysis data which indicates acceptable purity. Elemental analysis: Calcd. for $C_{22}H_{22}O_6$: C, 69.19; H, 5.80; Found: C, 69.10; H, 5.94. Figure 1 shows the synthesis of alpha-methyl curcumin.

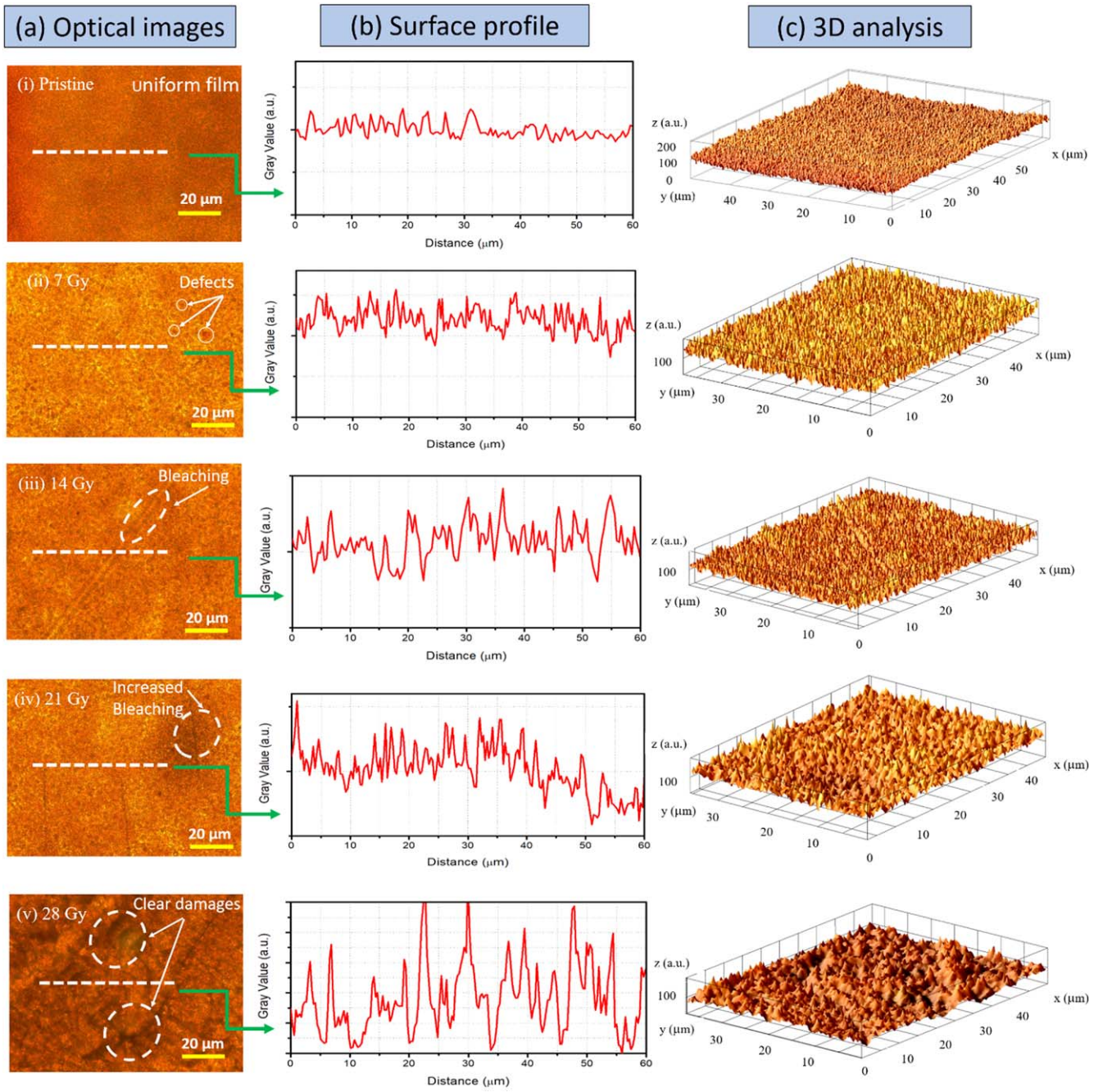

Figure 2. Surface morphology of alpha-methyl curcumin: PMMA sample: (a) showing the optical images of the sample in the pristine case and under irradiation for increasing γ-ray dose from top to bottom, (b) the surface profile of the selected white dashed line in (a). (c) Is the 3D analysis of the entire surface of the film in (a).

2.2. Preparation of sample

The thick films of alpha-methyl curcumin: doped by the poly (methyl methacrylate) (PMMA) were prepared by dissolving 8 mg of alpha-methyl curcumin in 1 ml of chloroform (CF) and 100 mg PMMA in 1 ml of chloroform (CF). After that, the dissolved solutions were stirred for 10 min on a hot plate, the solution then moved to sonicator for 30 min. After the material have completely dissolved in CF the solution of alpha-methyl curcumin was mixed with PMMA solution and stirred again for 15 min to generate a homogenous solution. Then, a drop cast method was used to prepare a thick film from the alpha-methyl curcumin: PMMA and the films were left overnight to make sure that the solvent slowly evaporated from the mixture. A digital micrometer (Leybold-heraeus, Germany) was used to measure the film's thickness and found it be 60 μm.

2.3. Irradiation of sample

^{137}Cs is the source for γ-ray used in the present study, it emits energy of 662 keV with a dose rate of 48 Rad min^{-1}. This source is available in the Department of Physics, College of Education for Pure Sciences, University of Basrah, Iraq. The

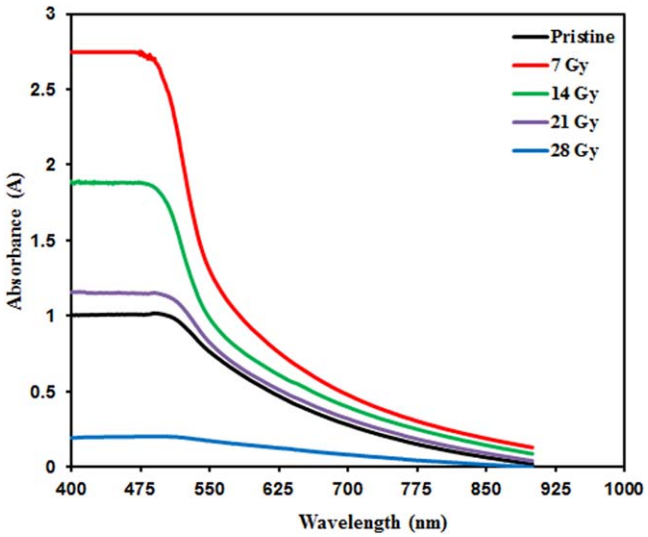

Figure 3. The UV–visible absorbance (*A*) against wavelength of the alpha-methyl curcumin: PMMA the pristine film and the γ-irradiated films with different doses.

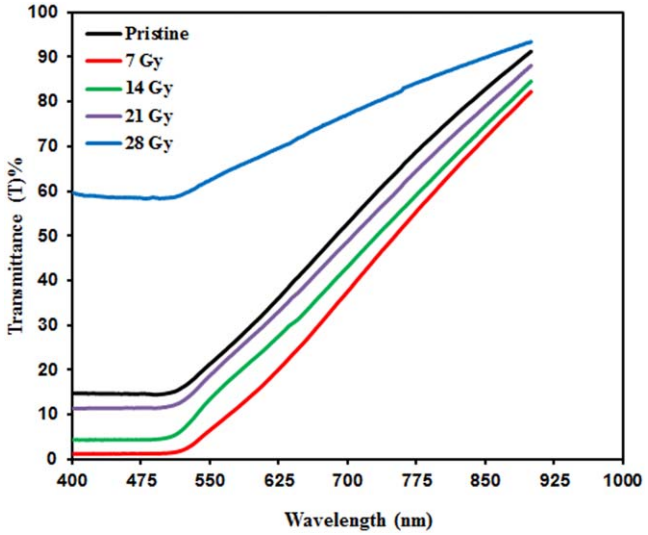

Figure 4. The variation of the transmittance (*T*) % against wavelength of the alpha-methyl curcumin: PMMA film pristine and the γ-irradiated films to different doses.

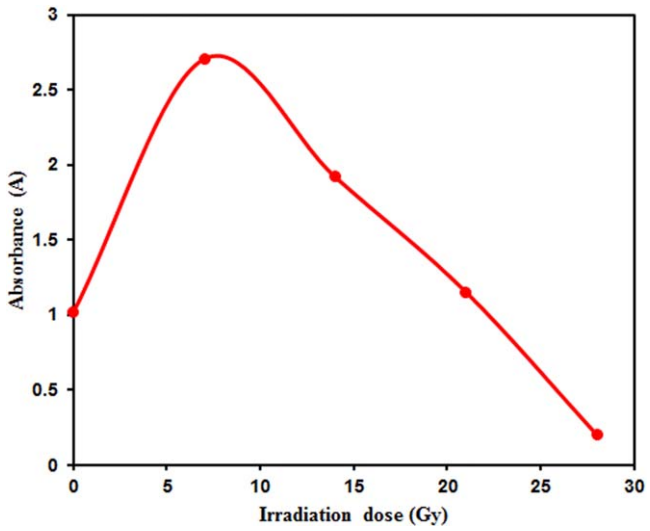

Figure 5. The variation of the absorbance (*A*) against the γ-irradiation dose for the alpha-methyl curcumin: PMMA film.

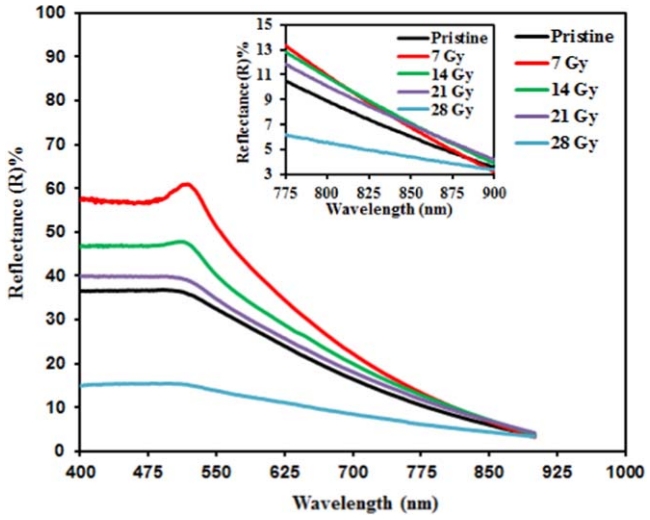

Figure 6. The variation of the reflectance, (*R*)%, against wavelength of the alpha-methyl curcumin :PMMA film pristine and the γ-irradiated to different doses. Inset is the magnification of reflectance curves in the 775–900 nm range.

sample was irradiated with the γ-ray for different times, viz., 14.58, 25.16, 43.75 and 58.33 min, i.e. doses of (7, 14, 21 and 28) Gy, respectively. Post each irradiation, an image was taken to the samples using the optical microscope (Leica DM 500) to determine the changes in the surface profile of the films.

2.4. Surface morphology analysis of the samples

The characterization of surface morphology of the pristine and the γ-irradiated samples with different doses (7, 14, 21 and 28) Gy were studied using an optical microscope along with open source Image J software to analyze the taken images by the optical microscope. Figure 2(a) shows the pristine and the γ-irradiated samples surface images. As can be seen in figure 2(a)(i), the pristine film is smooth, homogeneous and uniform. It can also be seen that the material (alpha-methyl curcumin and PMMA) is distributed regularly all over the substrate without any noticeable cracks, defects or pinholes. However, the film irradiated with 7 Gy γ-dose, as displayed in figure 2(a)(ii), shows defects on its surface and the color of the film changes from orange to yellowish-orange. Additionally, pinholes are clearly appeared on its surface with different shapes and sizes. These changes in the surface are due to the effect of γ radiation on the sample. When the dose was increased to 14 Gy, the film obviously shows a black line an indication of a chemical bleaching process on the surface (see figure 2(a)(iii)). The appearance of cracks and a black area on the film's surface indicates an increase in the area of bleaching of the irradiated sample with 21 Gy γ-dose as evident from figure 2(a)(iv). Clear damages occurred in the width of the cracks and the

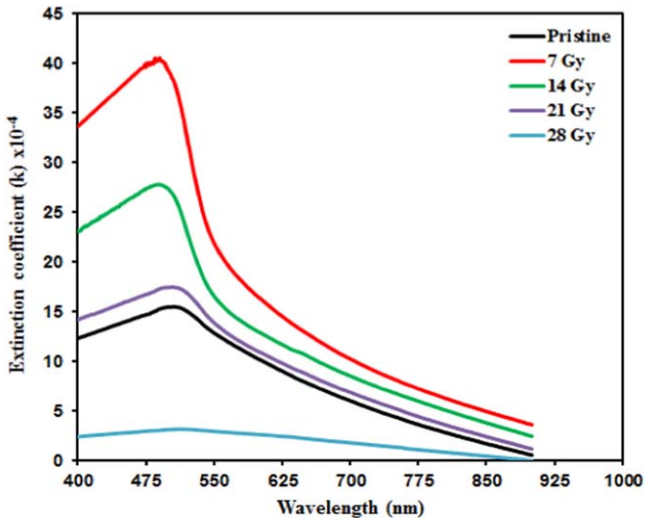

Figure 7. The variation of the extinction coefficient, k, against wavelength of the alpha-methyl curcumin: PMMA film the pristine and the γ-irradiated to different doses.

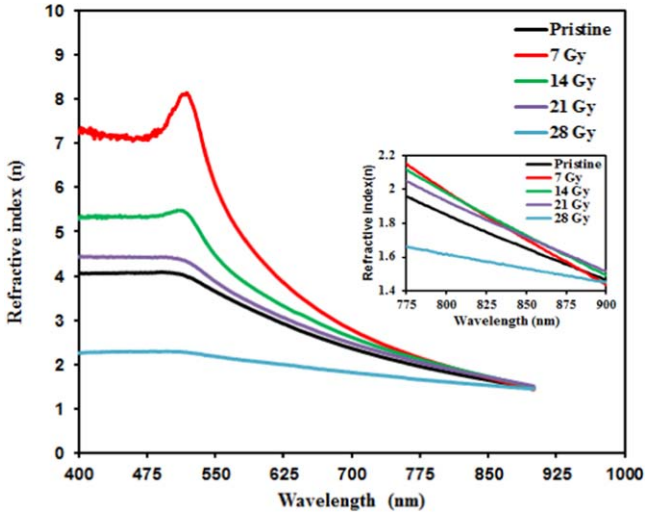

Figure 8. The variation of the refractive index, n, against wavelength of the alpha-methyl curcumin :PMMA film pristine and the γ-irradiated to different doses. Inset is the magnification of refractive index in the 775–900 nm range.

emergence of a larger number of black areas as the dose increased to 28 Gy, which confirms that a large proportion of the irradiated sample has been exposed to bleaching, as shown in figure 2(a)(v). The surfaces of the films were studied using Image J software to identify the changes occurred on their surfaces as the dose increased. Figure 2(b) from, top to bottom, shows the surface profile of the selected area of the original film (dashed white line). Based on the generated plots, it is clearly revealed that the gray scale of the sample increased which further confirmed that the cracks, defects, and pinholes becomes deeper as the sample exposed to a higher dose. The 3D analysis (figure 2(c) from top to bottom) is also indicates that these changes on the surface occurred due to the high γ- dose. The surface profile and the 3D analyses (figures 2(b) and (c)) are supportively confirmed the

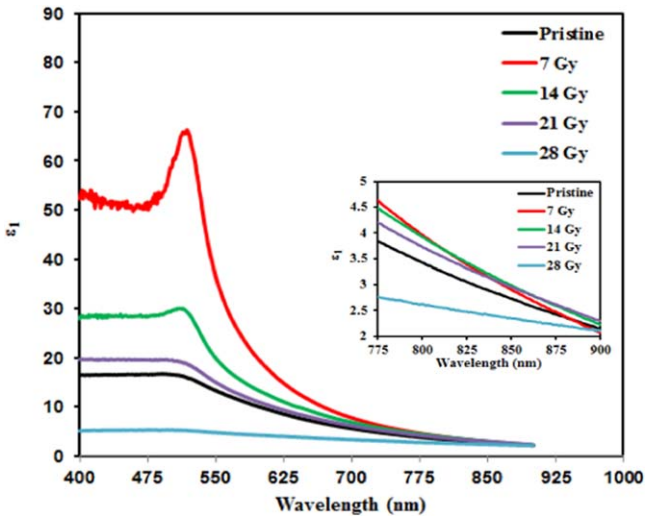

Figure 9. The variation of the real part of the dielectric constant, ε_1, against wavelength, of the alpha-methyl curcumin: PMMA film pristine and the γ-irradiated to different doses. Inset is the magnification of real part of the dielectric constant in the 775–900 nm range.

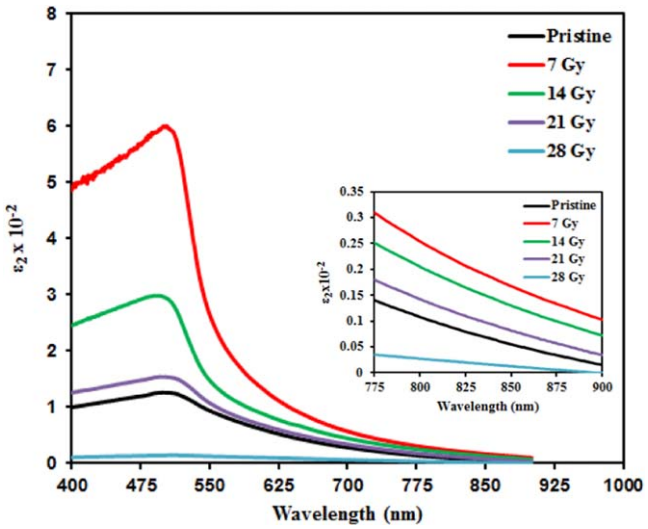

Figure 10. The variation of the imaginary part of the dielectric constant, ε_2, against wavelength, for the alpha-methyl curcumin: PMMA film pristine and the γ-irradiated to different doses. Inset is the magnification of imaginary part of the dielectric constant in the 775–900 nm range.

changes in the surface morphology in the optical images of the samples post exposed to γ-irradiation.

2.5. UV–visible spectroscopic study

Optical measurements of the pristine and the γ-irradiated samples were performed using UV–visible spectrophotometer (Jenway-England-6800) with a double beam in the wavelength range 400−900 nm at room temperature.

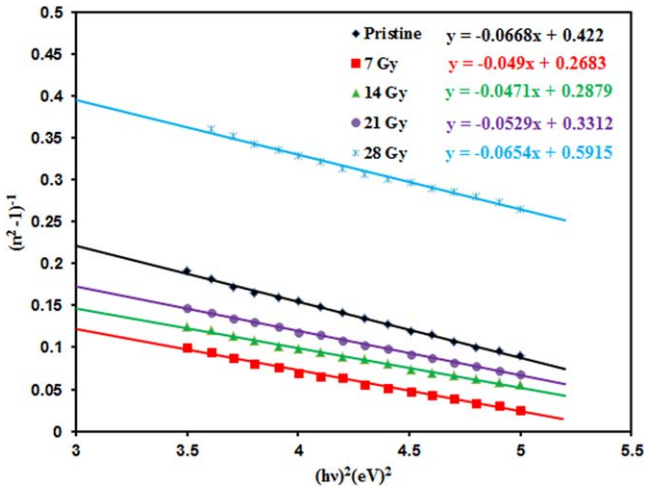

Figure 11. The variation of $(n^2-1)^{-1}$ against $(h\nu)^2$ of the alpha-methyl curcumin: PMMA film pristine and the γ-irradiated to different doses.

3. Results

The absorbance, A, and the transmittance, T, measurements of the pristine and the γ-irradiated samples at the four mentioned doses, are shown in figures 3 and 4 respectively. From figure 3 it can be seen that the absorption differ when it was exposed to γ radiation, also it can be seen that the absorptions of doses 7, 14, 21 Gy are higher than the pristine case while for dose 28 Gy it is lower than the pristine . Figure 5 displays the relation between the absorbance and the radiation dose at the wavelength 490 nm. The choice of this wavelength is based on the fact that the pristine has maximum absorption at this wavelength. It can be seen from the curve of figure 5 that the absorption of the sample increases for irradiation dose of 7 Gy, then decreases for higher doses but still higher than the pristine sample and finally decreases sharply at the dose 28 Gy.

As for the transmittance, from figure 4, it's behavior is inverse compare to the absorbance, where the transmittance increase with increased dose but it is lower than the pristine while it is higher than for dose 28 Gy compare to the pristine. The increase in the absorbance and the decrease in the transmittance post the irradiation of the sample with 7 Gy γ-dose may be due to changes in the surface roughness and created defects in the sample, as a result of sample exposure to high dose of γ radiation. Since the absorbance and transmittance depends mainly on the material structure, surface roughness and defects [63], as it is noted from section 2.4, the surface of the sample has changed and become more rough, also the formation of defects post-exposure to γ radiation, therefore the absorbance increases and transmittance decreases as the sample exposed to 7 Gy γ-dose. The decrease in the absorbance and the increase in transmittance for 14 and 21 Gy radiation doses are attributed to the bleaching process occurred (see figure 2(a)). Owe to the bleaching process at 21 Gy dose larger parts of the sample included compared to the 14 Gy radiation dose, this leads to a decrease in the absorbance and an increase in the transmittance of the former case more than the latter one. For the 28 Gy dose, it is noticed that large parts of the sample have been damaged due to the bleaching process (see figure 2(a)(v)), therefore the absorbance becomes lower and the transmittance becomes larger compared to the pristine and to the other γ-irradiated doses cases.

The reflectance, R, the absorption coefficient, α, the extinction coefficient, k, the refractive index, n, and the real, ε_1, and the imaginary, ε_2, parts of the dielectric constant of the pristine and the γ-irradiated samples can be obtained using the spectra of absorbance and transmittance and the following relations [64]

$$R = 1 - \sqrt{T\exp(A)}, \tag{1}$$

$$\alpha = 2.303\frac{A}{L}, \tag{2}$$

$$k = \frac{\alpha\lambda}{4\pi}, \tag{3}$$

$$n = \frac{1+R}{1-R} + \sqrt{\frac{4R}{(1+R)^2} - k^2}, \tag{4}$$

$$\varepsilon_1 = n^2 - k^2, \tag{5}$$

$$\varepsilon_2 = 2nk,$$

where L and λ are the sample thickness and the wavelength respectively. Figures 6–10 shows variations of R, k, n, ε_1, ε_2, against wavelength for the pristine and the γ-irradiated samples. Likewise absorbance, A, it is observed that R, k, n, ε_1 and ε_2 values for γ-irradiated with doses of 7, 14 and 21 Gy samples are higher compare to the pristine sample, while for the dose 28 Gy they are lower than that of the pristine sample. Also it is observed from figure 6 that the reflectance decreases with increasing dose up to 21 Gy compare to the pristine while it is lower for the dose 28 Gy. From the figure 7 it can be seen that the extinction coefficient increase with the increase of dose up to 21 Gy compare to the pristine case then it is lower compare to the pristine for the dose 28 Gy. The refractive index is higher than the pristine case for doses 7–21 Gy, but decreases lower than the pristine at higher dose as can see in figure 8. The same behavior is noticed for the real and imaginary parts of the dielectric constant (see figure 9). Insets in figures 6, 8–10 are the magnification of parts of the reflectance, refractive index, real and imaginary parts of the dielectric constant variations against wavelength in the 775–900 nm range. As the wavelength increase the reflectance, R, stay constant in the wavelength range 400–485 nm then increases smoothly at $\lambda = 525$ nm then decreases almost exponentially for $\lambda > 525$ nm for the pristine and the irradiated samples. The same behavior is seen for the refractive index, n, and the real part of the dielectric constant, ε_1. The extinction coefficient, k, and the imaginary part of the dielectric constant, ε_2, both increases for increasing the wavelength up to $\lambda = 485$ nm then decreases almost sharply.

Based on equation (7) [65] the dispersion energy parameter, E_d, for the pristine and the γ-irradiated samples can be

Table 1. The values of the dispersion energy parameter, E_d, the single-oscillator energy, E_0, the static refractive index, n_o, the linear optical susceptibility, $\chi^{(1)}$, the third-order nonlinear optical susceptibility, $\chi^{(3)}$), and the nonlinear refractive index, n_2, of the pristine and the γ-irradiated alpha -methyl curcumin: PMMA film.

Gamma dose (Gy)	E_d (eV)	E_0 (eV)	n_0	$\chi^{(1)}$	$\chi^{(3)} \times 10^{-12}$ (esu)	$n_2 \times 10^{-12}$ (esu)
Pristine	5.955	2.513	1.835	0.188	0.215	4.416
7	8.576	2.301	2.174	0.296	1.315	22.802
14	8.451	2.433	2.115	0.276	0.992	17.681
21	7.554	2.502	2.004	0.240	0.566	10.647
28	5.037	3.007	1.640	0.134	0.055	1.264

obtained

$$(n^2 - 1)^1 = \frac{E_0}{E_d} - \frac{1}{E_0 E_d}(h\upsilon)^2, \tag{7}$$

where E_0, h, ν are single-oscillator energy, the Planck's constant and the frequency of incident photon respectively. The values of E_0 and E_d for the pris tine and the γ-irradiated samples can be obtained, via drawing a relation between $(n^2-1)^{-1}$ as a function of $(h\nu)^2$. Figure 11 displays variation of $(n^2-1)^{-1}$ against $(h\nu)^2$.

The intersection of each straight line with the y axis resulting from the plot gives value equals to (E_0/E_d), and the slopes of the straight lines equals to $(-1/E_0E_d)$. The calculated values of E_0 and E_d for the pristine and the γ-irradiated samples are given in table 1. The values of E_0 and E_d can be used subsequently to evaluate the values of the static refractive index, n_0, which represent the refractive index at zero photon energy for the pristine and the γ-irradiated samples, can be determined via the following equation [65]

$$n_0^2 = \left(1 + \frac{E_d}{E_0}\right). \tag{8}$$

The values of the static refractive index, n_0, for the pristine and the γ-irradiated samples calculated using equation (8) are listed in table 1.

The linear optical susceptibility, $\chi^{(1)}$, the third-order nonlinear optical susceptibility, $\chi^{(3)}$, and the nonlinear refractive index, n_2, of the pristine and the γ-irradiated samples can be evaluated using the following relations [66]

$$\chi^{(1)} = \frac{E_d}{4\pi E_0}, \tag{9}$$

$$\chi^{(3)} = 1.7 \times 10^{-10}(\chi^{(1)})^4(\text{esu}), \tag{10}$$

$$n_2 = \frac{12\,\pi\,\chi^{(3)}}{n_0}(\text{esu}). \tag{11}$$

The computed values of $\chi^{(1)}$, $\chi^{(3)}$ and n_2 are listed in table 1. As can be seen in table 1 that the value of dispersion energy for the samples increases for radiation dose 7 Gy and decreases for radiation doses 14, 21 but still higher than the pristine sample, while for the radiation dose 28 Gy it became lower than the pristine case. Similar behaviors are observed for the static refractive index, n_0, the linear optical susceptibility, $\chi^{(1)}$, the third-order nonlinear optical susceptibility, $\chi^{(3)}$, and the nonlinear refractive index, n_2. The opposite is true for single-oscillator energy, E_0. Since the absorption increased with the increasing of γ-ray dose compare to the pristine case so that the parameters listed in the table 1 all increased sharply as the absorption does then decreased slowly.

It is known that many photonic and nonlinear optical devices needs materials with high values of the refractive index, n, the nonlinear refractive index, n_2, and the third order nonlinear optical susceptibility, $\chi^{(3)}$, [67, 68] and since the alpha-methyl curcumin: PMMA film under irradiation with γ-ray dose of 7 Gy shows high values of these parameters, this makes it suitable for photonic and nonlinear optical applications.

4. Conclusion

In this work, the curcuminoid alpha-methyl curcumin was prepared with the aid of ultrasonic waves. Alpha-methyl curcumin: PMMA film was prepared using casting method. Optical microscopy and Image J software program were used to investigate the surface morphology of the obtained film. The absorbance and the transmittance data which were obtained at room temperature by using UV–visible spectrophotometer are used to determine the optical parameters of the sample. The table 1: the values of the dispersion energy parameter, E_d, the single-oscillator energy, E_0, the static refractive index, n_0, the linear optical susceptibility, $\chi^{(1)}$, the third-order nonlinear optical susceptibility, $\chi^{(3)}$, and the nonlinear refractive index, n_2, of the pristine and the γ-irradiated alpha -methyl curcumin: PMMA film. The influence of γ-ray with different doses (7, 14, 21 and 28 Gy) on optical parameters of the alpha-methyl curcumin: PMMA film was studied. It was found that the absorbance, A, the reflectance, R, the extinction coefficient, k, the refractive index, n, the real, ε_1, and the imaginary, ε_2, parts of the dielectric constant, the nonlinear refractive index, n_2, the linear optical susceptibility, $\chi^{(1)}$ and the third-order nonlinear optical susceptibility, $\chi^{(3)}$, increased with the increased dose of the γ ray, where the increase is larger for the radiation dose 7 Gy and less for radiation dose 21 Gy, but for the dose 14 Gy is in the middle. As for radiation dose 28 Gy, it was found that the values of these optical parameters are less than the pristine sample. The objective of the current research is achieved by finding a new material that possesses high nonlinear optical properties and it is possible to improve these properties by exposing them to the appropriate dose of γ radiation. It is also found that the

radiation dose of 7 Gy is the optimum dose for the sample to show better properties. The results obtained of the alpha-methyl curcumin: PMMA film makes it good candidate for the use in photonic applications.

ORCID iDs

Qusay M A Hassan https://orcid.org/0000-0002-8941-6816
Ahmed S Al-Asadi https://orcid.org/0000-0001-6598-6286
Bahjat A Saeed https://orcid.org/0000-0002-0288-5389

References

[1] Manickasundaram S, Kannan P, Kumaran R, Velu R, Ramamurthy P, Hassan Q M A, Palanisamy P K, Senthil S and Narayanan S S 2011 Holographic grating studies i[n pendant xanthene dyes containing poly (alkyloxymethacrylate)s *J. Mater. Sci., Mater. Electron.* **22** 25–34
[2] Manickasundaram S, Kannan P, Hassan Q M A and Palanisamy P K 2008 Azo dye based poly (alkyloxymethacrylate)s and their spacer effect on optical data storage *J. Mater. Sci., Mater. Electron.* **19** 1045–53
[3] Dneprovskii V S, Furtichev A I, Klimov V I, Li S, Nazvanova E V, Okorokov D K and Vandishev U V 1988 Nonlinear optical properties of CdS and optical bi-stability *Phys. Stat. Sol.* **150** 839–44
[4] Al-Mudhaffer M F, Al-Ahmad A Y, Hassan Q M A and Emshary C A 2016 Optical characterization and all-optical switching of benzenesulfonamide azo dye *Optik* **127** 1160–6
[5] Al-Asadi A S, Hassan Q M A, Abdulkader A F, Mohammed M H, Bakr H and Emshary C A 2019 Formation of graphene nanosheets/epoxy resin composite and study its structural, morphological and nonlinear optical properties *Opt. Mater.* **89** 460–7
[6] Abdulkader A F, Hassan Q M A, Al-Asadi A S, Bakr H, Sultan H A and Emshary C A 2018 Linear, nonlinear and optical limiting properties of carbon black in epoxy resin *Optik* **160** 100–8
[7] Hussain M S, Hassan Q M A, Badran H A and Emshary C A 2013 Synthesis, characterization and third-order nonlinear optical properties of schiff base dimer *Int. J. Indus. Eng. Technol.* **3** 57–64
[8] Ali Q M and Palanisamy P K 2007 Optical phase conjugation by degenerate four-wave mixing in basic green 1 dye-doped gelatin film using He–Ne laser *Opt. Laser Technol.* **39** 1262–8
[9] Ali Q M and Palanisamy P K 2006 Z-scan determination of the third-order optical nonlinearity of organic dye nile blue chloride *Mod. Phys. Lett.* B **20** 623–32
[10] Hassan Q M A 2018 Study of nonlinear optical properties and optical limiting of acid green 5 in solution and solid film *Opt. Laser Technol* **106** 366–71
[11] Sultan H A, Hassan Q M A, Bakr H, Al-Asadi A S, Hashim D H and Emshary C A 2018 Thermal-induced nonlinearities in rose, linseed and chamomile oils using CW visible laser beam *Can. J. Phys.* **96** 157–64
[12] Hassan Q M A 2017 Investigation on the nonlinear optical properties and optical power limiting of parsley oil *Int. J. Photo. Opt. Technol.* **3** 17–20
[13] Hassan Q M A, Sultan H A, Al-Asadi A S, Bakr H, Hashim D H and Emshary C A 2018 Diffraction ring patterns and Z-scan measurements of nonlinear refractive index of khoba vegetable oil *J. Basrah Res. (Sciences)* **44** 47–63
[14] Hassan Q M A, Sultan H A, Baker H, Hashim D H and Emshary C A 2017 Diffraction patterns and nonlinear optical properties of Henna oil *J. Coll. Edu. Pure Sci.* **7** 90–103
[15] Hassan Q M A, Sultan H A, Bakr H, Ali I M, Hassan R M and Emshary C A 2018 Estimating the nonlinear refractive index of 10W30 oil using visible low power laser beam *Researcher* **10** 46–51
[16] Hassan Q M A, Bakr H, Sultan H A, Hassan R M and Emshary C A 2017 Evolution of far-field diffraction patterns and nonlinear optical properties of SAE 70 oil *Int. J. Appl. Nat. Sci.* **6** 181–8
[17] Emshary C A, Sultan H A, Hassan Q M A and Bakr H 2019 Nonlinearities of a brake fluid using low visble laser beam *Int. J. Phys. Appl. Sci.* **6** 42–53
[18] Bakr H, Hassan Q M A, Sultan H A and Emshary C A 2019 Diffraction ring patterns and Z-scan measurements of the nonlinear refraction index of 5W20 oil *J. Coll. Edu. Pure Sci.* **9** 226–32
[19] Marudhu G, Krishnan S and Samuel P 2013 Optical, thermal and mechanical studies on nonlinear optical material diglycine barium chloride monohydrate (dgbcm) single Crystal *J. Nonlinear Opt. Phys. Mater.* **22** 1350043
[20] Mousa A O, Kadhim Y H and Naser B A 2016 Study of nonlinear optical properties of nematic liquid crystal materials *Int. J. Phys. Res.* **6** 17–24
[21] Gamernyk R, Periv M and Malynych S 2014 Nonlinear-optical refraction of silver nanoparticle composites *Opt. Appl.* **44** 389–98
[22] Al-Nasir E A, Al-Ahmad A Y, Hussein A A, Ali Q M, Sultan A A and Al-Mowali A H 2013 Low optical limiting and nonlinear optical properties of vanadyl phthalocyanine using a CW laser *Chem. Mater. Res.* **3** 18–25
[23] Kadhum A J, Hussein N A, Hassan Q M A, Sultan H A, Al-Asadi A S and Emshary C A 2018 Investigating the nonlinear behavior of cobalt (II) phthalocyanine using visible CW laser beam *Optik* **157** 540–50
[24] Elias R S, Hassan Q M A, Sultan H A, Al-Asadi A S, Saeed B A and Emshary C A 2018 Thermal nonlinearities for three curcuminoids measured by diffraction ring patterns and Z-scan under visible CW laser illumination *Opt. Laser Technol.* **107** 131–41
[25] Margar S N and Nagaiyan S 2016 Nonlinear optical properties of curcumin: solvatochromism-based approach and computational study *Mol. Phys.* **114** 1–13
[26] Sultan H A, Hassan Q M A, Al-Asadi A S, Elias R S, Bakr H, Saeed B A and Emshary C A 2018 Far-field diffraction patterns and optical limiting properties of bisdemethoxycurcumin solution under CW laser illumination *Opt. Mater.* **85** 500–9
[27] Elias R S, Hassan Q M A, Emshary C A, Sultan H A and Saeed B A 2019 Formation and temporal evolution of diffraction ring patterns in a newly prepared dihydropyridone *Spectrochim. Acta* A **223** 117297
[28] Imran A, Badran H A and Ali Hassan Q M 2014 Self diffraction and nonlinear optical properties for 2, 3-Diaminopyridine under cw illumination *IOSR J. Eng.* **4** 2278–8719.
[29] Hassan Q M A 2008 Nonlinear optical and optical limiting properties of chicago sky blue 6B doped PVA film at 633 nm and 532 nm studied using a continuous wave laser *Mod. Phys. Lett.* B **22** 1589–97

[30] Ali Q M and Palanisamy P K 2005 Investigation of nonlinear optical properties of organic dye by Z-scan technique using He–Ne laser *Optik* **116** 515–20

[31] Gholami-Kaliji S, Saievar-Iranizad E, Dehghani Z and Majles-Ara M H 2011 Influence of synthesis temperature on linear and nonlinear optical properties of water soluble luminescent $Cd_{1-x}Zn_xTe$ nanocrystals *Phys. Proc.* **19** 403–7

[32] Badran H A, Hassan Q M A and Imran A 2015 Large third order optical nonlinearity and optical limiting properties of a 3,4-diaminopyridine *J Mater. Sci.: Mater. Electron.* **26** 5958–63

[33] Badran H A, Abul-Hail R C, Shaker H S, musa A I and Hassan Q M A 2017 An all-optical switch and third-order optical nonlinearity of 3,4-pyridinediamine *Appl. Phys.* B **123** 31

[34] Badran H A, Qusay A I and Hassan, M A 2016 Thermal diffusivity of 2,3-Pyridinediamine determination by thermal blooming *Optik* **127** 2659–65

[35] Machnowski W, Gutarowska B, Perkowski J and Wrzosek H 2012 Effect of gamma radiation on the mechcanical properties and susceptibility to biodegradation of natural fibers *Tix. Res. J.* **0** 1–12

[36] Rani N S, Sannappa J, Demappa T and Mahadevaiah K 2013 Gamma radiation induced conductivity control and characterization of structural and thermal properties of hydroxyl propyl methyl cellulose (HPMC) polymer completed with sodium iodide (NaI) *Pel. Res. Lib.* **4** 195–219

[37] Eid S, Ebraheem S and Abdel-Kader N M 2014 Study the effect of gamma radiation on the optical energy gap of poly (vinyl alcohol) based ferrotitanium alloy films:Its possible use ir radiation dosimetry *Open J. Pol. Chem.* **4** 21–30

[38] Brostow. W, Castuno V M and Martinez-Barrera G 2005 Gamma irradiation effect on polystyrene + SBR blends: morphology and micro hardness *Polymer* **50** 657–62

[39] Arshak K and Korostynska O 2002 Gamma radiation dosimetry using tellurium dioxide thin film structure *Sensors* **2** 347–55

[40] Martel-Estrada S A, Santos-Rodrignes E, Olivas Armendariz I, Crnz-Zaragoza E and Martinez-perez C A 2014 The effect of radiation on the thermal properties of chitosan/mimosa tenniflora end chitosan/mimosa tenuiflora/ multiwalled carbon nanotubes (MWCNT) composites for bone tissue engineering *AIP Conf. Proc.* **1607** 55–64

[41] Darwish A A A, Issa S A M and El-Nahass M M 2016 Effect of gamma irradiation on structural, electrical and optical properties of nanostructure thin films of nickel phthalocyamine *Synth. Met.* **215** 200–6

[42] Kilic M, Karabul Y, Alkan U, Yagci O, Okutan M, Okutan M and Icelli O 2017 Gamma ray irradiation effect on mechanical and electrical properties of vleanic basalt mineral reinforced low density polyethylene films *Physicochem. Problems Miner. Process.* **53** 572–90

[43] Tahir K J 2017 Effect of gamma irradiation on optical properties of Cds thin film *J. Vniv. Ker.* **15** 49–55

[44] Song W, Song Q, Wu L and Yang L 2017 Effect of gamma irradiation on optical properties of aluminum dihydrogen triphosphate *J. Ser. Chem. Soc.* **82** 1111–21

[45] Ramya J R, Arul K T, Sathiamurthi P, Asokan K, Sing N R and Klkura S N 2018 Eahanced magnehe behavior and cell proliferation of gamma irradiated dual metal ions co-doped hydroxyapatite poly (methyl methacrylate) composite films *Reactive Funct. Polym.* **123** 34–43

[46] Al- Harbi W and Aly K A 2018 Effect of γ-radiation dose on the optical properties of $(AsTe)_x(GeSe_2)_{100-x}(x = 5)$ thin films *Chalcog. Lett.* **15** 75–81

[47] Mustapha N, Alkaoud A, Alyamani A and Idriss H 2018 Influence of gamma ray onto transparent indium tin oxide thin films *J. Ovo. Res.* **14** 225–33

[48] Babu B, Moharaj K, Chandrasekar S, Kumar N S and Mohanbabu B 2018 Effect of gamma radiation on structural, optical and electrical properties of nanostructured CdHgTe thin films *Nanosci. Rep.* **1** 26–31

[49] Salari M A, Odabs M, Guzeldir B and Salgam M 2018 The effect of gamma irradiation on structural and surface properties of ZnO thin films deposited on n-Si substrate *Int. J. Sci. Eng.* **9** 16–23

[50] Ramya J R *et al* 2019 Gamma irradiation poly((methyl methacrylate) reduced graphene oxide composite thin films *Composites* B **163** 34–43.

[51] Paula M, Diego I, Dionisio R, Vinhas G and Alves S 2019 Gamma irradiation effect on poly (aprolactone/ zinc oxide nanocomposite film *Polimeros* **29** 1–7

[52] Karmaker N, Islam F, Islam M N, Razzak M, Koly F A, Chowdhury A M S and Khau R A 2019 Fahrication and characterization of PVA-Gelatin _Nao crystalline cellulose based biodegradable film: effect of gamma irradiation *J. Res. Updates Polym. Sci.* **8** 7–14

[53] Elamin A A, Bashir A F, Ahmed R H and Abd Elgani R 2019 Effect of gamma ray on the optical properties of TiO_2 and ZnO thin films *Condens. Mater. Phys.* **132** 53386–91

[54] Nabiyev A, Linnik D S, Gorshkova Y E, Maharramav A M, Balasoiu M, Olejniczak A, Ivankov A, Kovalev Y S and Kuklin A I 2019 Influence of gamma irradiation on the morphological properties of HOPE+% ZrO_2 polymer nanocompsites *Rom. J. Phys.* **64** 603

[55] Lee W-H, Loo C-Y, Bebawy M, Luk F, Mason R S and Rohanizadeh R 2013 Curcumin and its derivatives: their application in neuropharmacology and neuroscience in the 21st century *Curr. Neuropharmacol.* **11** 338–78

[56] Wilken R, Veena M S, Wang M B and Srivatsan E S 2011 Curcumin: a review of anti-cancer properties and therapeutic activity in head and neck squamous cell carcinoma *Mol. Cancer* **10** 12

[57] Biswas S K 2016 Does the interdependence between oxidative stress and inflammation explain the antioxidant paradox *Oxid. Med. Cell. Longev.* **12** 569893

[58] Hewlings S J and Kalman D S 2017 Curcumin: a review of its' effects on human health *Foods* **6** 92

[59] Priyadarsini K I 2013 Chemical and structural features influencing the biological activity of curcumin *Curr. Pharm. Des.* **19** 2093–100

[60] Chiqnell C F, bilski P, Reszka K J, Motten A G, Sik R H and Dahl T A 1994 Spectral and photochemical properties of curcumin *Photochem. Photobiol.* **59** 295–302

[61] Manolova Y, Deneva V, Antonov L, Drakalska E, Momekova D and Lambov N 2014 The effect of thewater on the curcumin tautomerism: a quantitative approach *Spectrochim. Acta* A **132** 815–20

[62] Yingjie L, Ye B and Jie O 2011 Synthesis of some curcumin analogues under ultrasound irradiation *Adv. Mater. Res.* **332–334** 1623–6

[63] Pervez M F, Mia M N H, Hossain S, Saha S M K, Ali M H, Sarker P, Hossain M K, Matin M A, Hoq M and Chowdhury M A M 2018 Influence of total absorbed dose of gamma radiation onoptical bandgap and structural properties of Mg-doped zincoxide *Optik* **162** 140–50

[64] Al-Ahmad A Y, Hassan Q M A, Badran H A and Hussain K A 2012 Investigating some linear and nonlinear optical properties of the azo dye (1-amino-2-hydroxy naphthalin sulfonic acid-[3-(4-azo)]-4-amino diphenyl sulfone) *Opt. Laser Technol.* **44** 1450–5

[65] Sakr G B, Yahia I S, Fadel M, Fouad S S and Romčević N 2010 Optical spectroscopy, optical conductivity, dielectric properties and new methods for determining the gap states of CuSe thin films *J. Alloy Compd.* **507** 557–62

[66] Taha T A 2019 Optical properties of PVC/Al2O3 nanocomposites films *Polym. Bull.* **76** 903–18

[67] Oubaha M, Elmaghrum S, Copperwhite R, Corcoran B, McDonagh C and Gorin A 2012 Optical properties of high refractive index thin films processed at low-temperature *Opt. Mater.* **34** 1366–70

[68] Kohoutek T, Orava J, Sawada T and Fudouzi H 2011 Inverse opal photonic crystal of chalcogenide glass by solution processing *J. Colloid Interface Sci.* **353** 454–8